Use of Pulse-Energized Electrostatic Precipitator to Remove Submicron Particulate Matter in Exhaust Gas

Vishnu Thonglek[1] & Tanongkiat Kiatsiriroat[2]

[1]Graduate School, Chiang Mai University, Chiang Mai 50200, Thailand
[2]Department of Mechanical Engineering, Faculty of Engineering,
Chiang Mai University, Chiang Mai 50200, Thailand
Email: Vishnu_tn@hotmail.com

Abstract. An electrostatic precipitator (ESP) with negative pulse corona discharge for removal of submicron particles in the exhaust gas of thermal equipment such as boilers, burners or internal combustion engines is presented. A wire-cylinder ESP was designed and constructed for experimental testing at laboratory scale. The collection efficiency of submicron particles in the exhaust gas of a diesel burner under various dust loadings and gas velocities was investigated. The results were compared with those obtained from the conventional DC ESP technique. It was found that the pulse peak voltage supply could be set much higher than the sparking limit of the DC energized unit. Thus, the electric field density could be increased, which resulted in a higher collection efficiency. The higher pulse frequency also increased the collection efficiency, especially for submicron particles.

Keywords: *dc energized electrostatic precipitator; diesel exhaust gas; pulse-energized electrostatic precipitator; submicron particulate matter; submicron particle removal.*

1 Introduction

Emission control of fine particulate matters has been of great interest due to their serious effects on human health. Many countries have launched new emission regulations. For combustion chambers or furnaces, the existing concepts for controlling the particulate matter in exhaust gas are normally based on electrostatic precipitators (ESPs) due to their highly effective particle capture with low pressure drop. The mass collection efficiency of an ESP can reach over 90%. However, this technique is not suitable for submicron particles in the range of 0.1-1 μm and ultrafine particles with a size of less than 0.1 μm. These submicron particles are very harmful to human health. Therefore, a technique for enhancing submicron particle collection via a conventional ESP is needed.

In direct current (DC) electrostatic precipitation, it is rather difficult to charge ions on the submicron particles due to the extremely small size of the particles. For the entrainment, the collection efficiency of submicron particles drops sharply when the electrical resistivity of the particles drops below 10^2 ohm-m

Received September 18th, 2013, Revised February 6th, 2014, Accepted for publication April 11th, 2014.
 ISSN: 2337-5779, DOI: 10.5614/j.eng.technol.sci.2014.46.3.3

[1]. In this case, the efficiency cannot be increased by increasing the voltage due to the low electrical resistance of the submicron particles. Moreover, with moisture, an electrical breakdown may occur, which terminates particle capture [2].

Recently, a number of studies on pulse corona energization to generate non-thermal plasma (NTP) have been published. With this technique, an ESP can generate a much higher electron density than with DC energization and hence enhance particle charging due to the much larger mobility of the electrons [3]. As a result, the collection efficiency of submicron particles is improved. Zukeran, *et al*. [4] experimentally studied the ultrafine particle collection efficiency of ESP under DC and pulsed operating modes. The experimental results showed that the collection efficiency for DC applied voltage decreased with increasing dust loading when particle density was larger than 2.5×10^{10} particles/m^3 due to inefficient collection of ultrafine particles. However, under pulsed operation mode without DC bias, a high collection efficiency of ultrafine particles was obtained due to the enhancement of particle charging by electrons. Xu, *et al*. [5] have shown that the number of negatively charged particles was higher than the number of positively charged particles, which could reach a ratio of up to 2:1. Through theoretical analysis it was demonstrated that the positive short-pulse corona discharges included both steamer and corona discharges. Xue, *et al*. [6] have shown that most particles larger than 0.2 μm are negatively charged, while most particles smaller than 0.2 μm are positively charged. For a given operating condition, the particle penetration efficiency curve had the highest penetration efficiency for particles with a diameter near 0.2 μm and over 90% of PM2.5 could be collected in pulsed ESP. Sato, *et al*. [7] developed a PM electrostatic precipitator, integrating a duct pocket with a dielectric barrier discharge (DBD) device installed downstream. Carbon particles were oxidized by the barrier discharges and pulled into the high electric field region touching the mesh of the dust pocket. After operating the experiment for a period of up to 180 min, the collecting efficiency could be kept at an almost constant level of 99%.

This paper presents the design procedure for a wire-cylinder ESP and a laboratory unit that were constructed to study the effects of pulse-energized electrostatic precipitation on submicron particle capture in the exhaust pipe of a small diesel burner. Parameters affecting the collection efficiency, such as pulse duration, pulse frequency, pulse peak voltage and gas flow rate, were investigated.

2 Material and Methods

2.1 Design Procedure of Pulsed-Energized ESP

In an ESP design, particle collection efficiency is the first term to be considered, which can be estimated from [8].

$$\eta_f = 100\left(1\text{-}e^{\text{-De}}\right), \tag{1}$$

$$De = U_m \frac{A_c}{Q_g} \tag{2}$$

where η_f is the fractional collection efficiency, *De* is the Deutsch number, U_m is the migration velocity of a charged particle, A_c is the collection surface area, and Q_g is the gas flow rate.

When the charged particles in the gas stream are introduced into an electrostatic field, the Stokes drag force will be balanced by the electrostatic force, resulting in the migration velocity of a charged particle, U_m, which is given by

$$U_m = \frac{n_p e E_{ce} C_c}{3\pi\mu d_p}. \tag{3}$$

where n_p is the number of charge on the particle, e is the charge of the electron, E_{ce} is the electric field strength near the collecting electrode, C_C is the Cunningham slip factor, μ is gas viscosity, and d_p is particle diameter.

The total charge on the particle is the summation of the contributions from electric field and diffusion charging [9], which can be expressed as

$$n_p = \left(1 + 2\frac{\varepsilon\text{-}1}{\varepsilon+2}\right)\left(\frac{E_{ps} d_p^2}{4K_E e}\right)\left(\frac{\pi K_E e Z_i N_i t}{1+\pi K_E e Z_i N_i t}\right) + \frac{d_p k_B T}{2K_E e^2} \ln\left(1 + \frac{\pi K_E d_p \bar{c}_i e^2 N_i t}{2k_B T}\right). \tag{4}$$

where ε is the dielectric constant of the particle (for carbon black particles, ε = 3.0 [10]), E_{ps} is the pseudo-homogeneous electric field strength, Z_i is the ion electrical mobility (1.54×10^{-4} m /Vs at 100°C), K_E is the electric constant (9×10^9), k_B is the Boltzmann constant (1.38×10^{-23}J/K), $\bar{c}_i$ is the average ion thermal velocity (240 m/s), T is the gas temperature during charging time, and N_i is the ion concentration.

For this study, a wire cylinder electrode ESP as shown in Figure 1 was selected because of its simple geometry. A high-voltage power supply was connected to the discharge wire electrode while the collecting electrode was grounded. Operation started when the supplied voltage, *V*, was higher than the corona onset voltage, V_c.

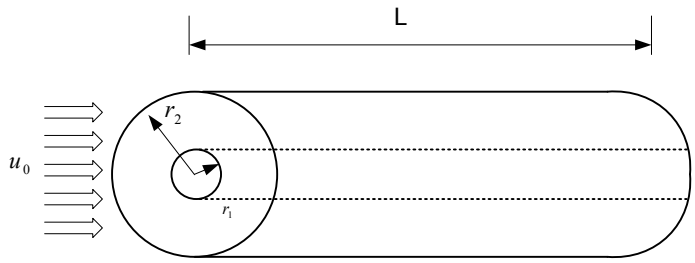

Figure 1 The wire-cylinder ESP configuration.

The ion concentration between the electrodes of the ESP is the main cause of particle charging. The particles are charged by the attachment of ions produced by the corona discharge. The ion concentration can be calculated from

$$\mathrm{N_i} = \frac{\mathrm{I}}{\mathrm{A_c e Z_i E_{ps}}}. \tag{5}$$

where $\mathrm{E_{ps}}$ is the strength of the electric field in the ESP, which is called pseudo-homogeneous electric field strength, given by

$$\mathrm{E_{ps}} \cong \frac{\mathrm{V}}{\mathrm{r_2}}. \tag{6}$$

The corona discharge current starts when the supplied voltage is higher than the corona onset voltage. After that, the whole process of the ESP mainly depends on the supplied voltage, V, and current I. The relation between V and I for corona discharge in an ESP is defined as

$$\mathrm{I} = \frac{8\pi \mathrm{L}\varepsilon_0 \mathrm{Z_i}}{\mathrm{r_2^2 \ln\left(\frac{r_2}{r_1}\right)}} \mathrm{V(V\text{-}V_c)} \text{when } \mathrm{V} > \mathrm{V_c}. \tag{7}$$

The corona onset voltage, V_c, can be calculated from

$$\mathrm{V_c} = \mathrm{E_c r_1 ln}\left(\frac{\mathrm{r_2}}{\mathrm{r_1}}\right). \tag{8}$$

The electric field strength $\mathrm{E_c}$ to generate a corona discharge can be calculated from [1].

$$\mathrm{E_c} = 31\delta\left[1 + \frac{0.308}{\sqrt{\delta \mathrm{r_1}}}\right]. \tag{9}$$

where δ is relative air density, which can be calculated from

$$\delta = \frac{298}{273+\mathrm{T}} \cdot \frac{\mathrm{P}}{760}. \tag{10}$$

where T is temperature and P is pressure of ambient air.

In a pulse-energized ESP, the pulse corona discharge generates free electrons that flow toward the collection electrode. When they encounter particles, particle charging occurs. The residual electric field, *E*, keeps driving the charged particles toward the collection electrode. In a negative corona, the positive ions in the active zone move back to the discharge wire, whereas the negative ions keep moving towards the collecting electrode. The negative ions have mobility $Z_i^- = 2.2 \times 10^{-4} \frac{m^2}{Vs}$[1], thus the transit time of an ion between the discharge wire, r_1, and the collecting electrode, r_2, at a distance of (r_2-r_1) can be calculated from

$$t_s = \frac{r_2 - r_1}{U_i}. \tag{11}$$

where t_s is the transit time of the ions and U_i is the ion drift velocity, defined as [11]

$$U_i = Z_i^- E. \tag{12}$$

The peak voltage duration, (t_d), which is the duration of generating the electric field, must be shorter than the transit time so that the ions will not reach the collecting electrode, otherwise, electrical breakdown will occur. Anyhow, even if ion generation is stopped, the negative ions in the gap will continue to move in the electrical field and form current. The time until the current has completely decayed is close to the ion transit time given in Eq. (11) [11]. Then, time period t_p of the power supply for the next supplied pulse peak voltage should be

$$t_p = t_d + t_s. \tag{13}$$

To prevent the occurrence of electrical breakdown, the maximum pulse frequency of the supplied voltage, *f*, must be over $1/t_p$.

The above equations were used to evaluate the values for designing an experimental unit. The steps for calculation are shown in Figure 2. For our experimental ESP, a collection efficiency of 95% was prescribed. The average gas velocity in the designed ESP was about 1 m/s. The volumetric gas flow rate was 0.003 m^3/s, the temperature of the gas entering the ESP was about 35°C, and the pressure was 1 atm. The designed length of the ESP was 0.5 m. Bakelite and PVC pipe were used as electrical insulation between the wire and collection electrodes as well as the outer chassis of the ESP, so that the maximum voltage of 15 kV could be used. Details of the design criteria for the ESP are given in Table 1.

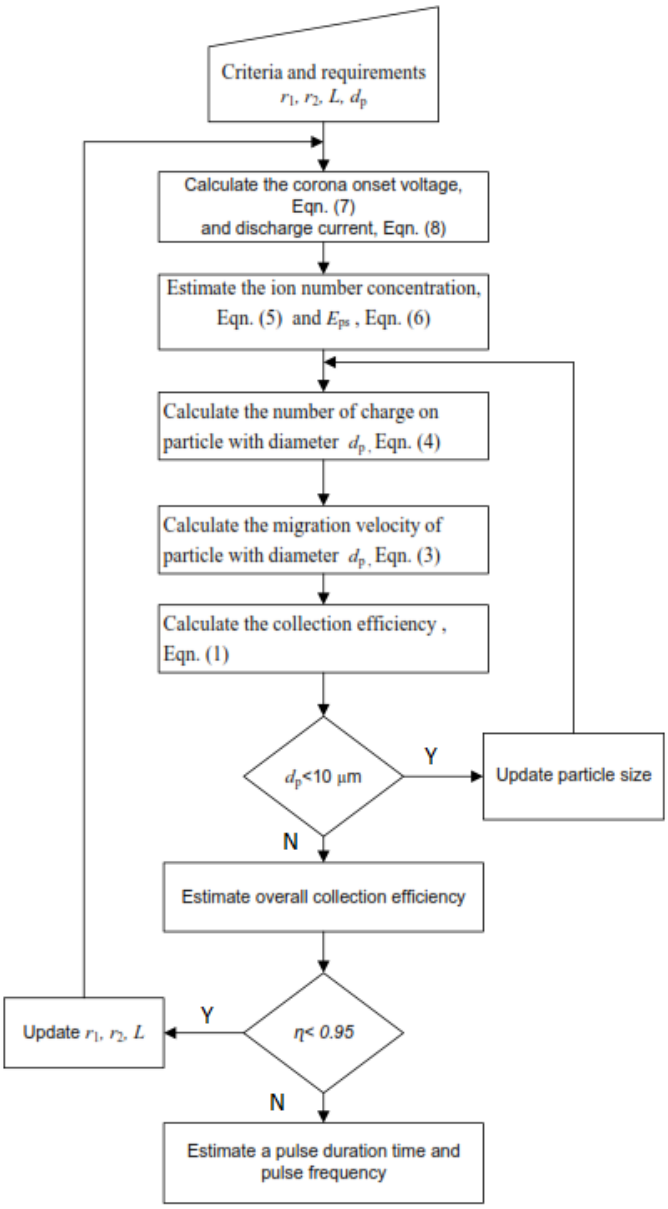

Figure 2 Flowchart for evaluating the values for designing.

Since the collection efficiency for the design was selected to be 95%, the dimensions of the stainless tube could be 100 mm outer and 90 mm inner diameter, while the discharge tungsten wire diameter was 0.3 mm. This value provided a corona onset voltage of 3.5 kV, while the distance between the

electrodes was r_2-$r_1 \approx r_2 = 45$ mm , which resulted in a drift velocity of 73 m/s in an electric field of 333 kV/m. The typical transit time was 613.66 μs. In industrial ESPs, the estimated pulse duration is less than 10 μs [12]. After a recovery period, the gas is ready again to support the next pulse, which provides a maximum frequency of 1.4 kHz. Based on this concept, a high-voltage pulse generator was developed of which the pulse duration was about 10 μs and the amplitude 15 kV.

Table 1 Criteria and requirements used in the design of the wire-cylinder ESP.

Parameter	Values
Air temperature, T(K)	400
Applied voltage negative pulse (kV)	15
Collection efficiency (%)	95
Gas velocity u_g(m/s)	1
Pressure (atm)	1

2.2 Experimental Setup

Figure 3 shows the experimental setup, which consisted of a soot generator, an ESP, and a wire cylinder electrode ESP.

A stainless steel cylinder with a 90 mm inside diameter and 500 mm length was used as the collection electrode. The discharge electrode was made of tungsten wire with a 0.3 mm diameter and was located along the center of the stainless steel cylinder. The distance between the discharge wire and the collecting electrode was 45 mm.

Exhaust gas of diesel combustion from a Bunsen burner (soot generator) was introduced to the test unit. The inlet concentration of the particulate matter in the exhaust gas was adjusted to be 5×10^5 particle/cm^{-3} and the speed of the airflow was controlled by a downstream blower with a speed controller.

The pulsed power supply produced a high-voltage pulse according to the principle of resonant charging. The 12 V DC voltage from a battery could be stepped up to 15 kV by a pulse transformer with a frequency range of around 1 to 60 kHz. Rise time and pulse width were 400 ns and 10 μs, respectively. After that the high-voltage waveform from the pulse transformer was rectified to be DC by a high-voltage diode before supplying it to the ESP. The average current flow to the ESP was measured by a true-RMS digital multimeter to measure the voltage between the collecting electrode and the ground. Both the average and peak voltage across the electrode gap were measured with a high voltage probe. The testing conditions of the ESP are given in Table 2.

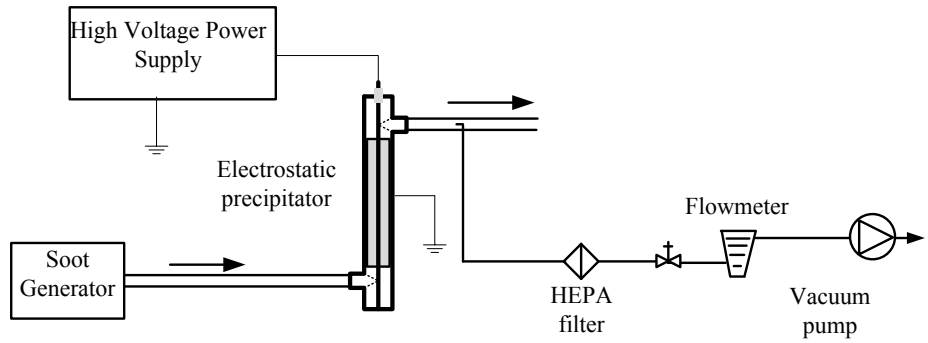

(a) The experimental setup.

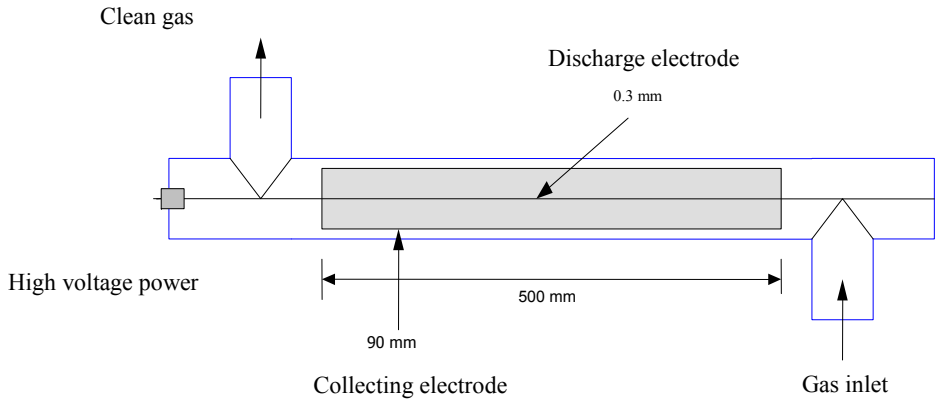

(b) The wire-cylinder ESP configuration for the experiments.

Figure 3 Schematic diagrams of the experimental setup and the wire-cylinder ESP.

Table 2 Testing conditions of the constructed ESP.

Parameter	Value
Diameter of discharge wire (mm)	0.3
Diameter of tube (mm)	90
Length of tube (mm)	500
Air temperature, T (K)	308
Supplied voltage negative pulse (kV)	0-15
Particle diameter, d_p(micron)	0.1-100
Gas velocity, u_g(m/s)	0.5,1,1.5,2
Pulse duration (μs)	10
Pulse frequency (kHz)	1,20,40, 60

To be able to measure the number of particles in the exhaust gas, the gas has to be diluted by mixing it with clean air, after which the mixed gas is sent to a laser particle counter (LPC). The LPC is able to measure the number density of particles that have a size between 0.3 and 5 μm. The fractional collection efficiency, η_f, based on particle number concentration, can be evaluated from the number concentrations upstream and downstream of the ESP. It can be defined as

$$\eta_f(d_p) = 1\text{-}\frac{N_{out}(d_p)}{N_{in}(d_p)}. \quad (14)$$

where $N_{in}(d_p)$ and $N_{out}(d_p)$ are the number concentrations for particles having a size of d_p, upstream and downstream of the ESP, respectively.

The collection efficiency on a mass basis of the ESP was evaluated for one-hour operation with a high efficiency particulate-free air (HEPA) glass fiber filter with a diameter of 47 mm. The exhaust gas downstream of the ESP was sampled every 10 min during operation. The gas flow rate was set to be 10 L/min by a modulating valve. A flow meter was used to measure the gas flow that was sucked out by a vacuum pump. The filters were treated prior to use by placing them in a desiccator at room temperature with 50-60% of relative humidity using a sodium dichromate solution as the controller for at least 24 hours before and after sampling. The filters were then weighed using a precision digital weighing meter. The weight of the particles collected on the filter was measured every 10 min. The collection efficiency (all particle sizes) can be evaluated from the mass difference on the HEPA filters upstream and downstream of the ESP as

$$\eta_t = 1\text{-}\frac{M_{out}}{M_{in}}. \quad (15)$$

where M_{in} and M_{out} are the total masses of all particle sizes, upstream and downstream of the ESP channel, respectively.

3 Result and Discussion

3.1 Voltage-Current Characteristics

Figure 4 shows the voltage-current characteristics of the ESP unit for DC ESP and pulse energized ESP at no dust loading. The time-average discharge current was increased with the applied voltage. Upon supplying a high negative voltage with the DC power supply, the corona occurred at an onset voltage of 3.2 kV, after which the current gradually increased in quadratic function with the voltage. When the supplied voltage was higher than 7 kV, a spark occurred between the tungsten wire and the inside cylindrical tube of the electrostatic

precipitator. However, when the high pulse power supply was used, the current gradually increased in quadratic form with the voltage similar to the energized negative DC supply, but electrical breakdown occurred at a higher value of the supplied voltage. The electrical breakdown occurred at around 8 kV, 10 kV, and 12 kV at pulse frequencies of 60 kHz, 40 kHz, and 20 kHz, respectively, whereas for the DC ESP it was at 7 kV. At low pulse frequencies, e.g. 1 kHz, the pulse peak voltage could rise up to more than 15 kV without any spark.

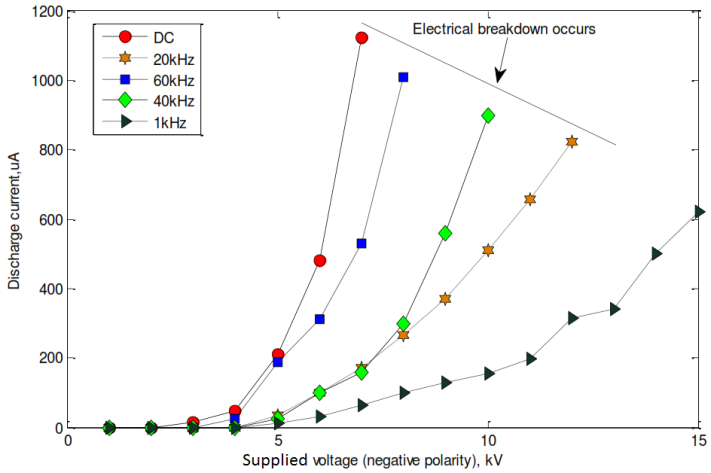

Figure 4 Voltage-current characteristics of the designed ESP for DC-energization and pulse-energization.

3.2 Effect of Pulse Frequency on Fractional Collection Efficiency

Experiments were carried out to investigate the effect of pulse frequency on fine particle collection efficiency. The measurements were made with a gas velocity controlled at about 0.5 m/s and the pulse peak voltage was kept constant at -10 kV. A laser particle counter was employed to measure the particle number concentration distributions for various particle sizes, ranging from 0.3 μm to 5 μm. The total number concentration of the particles was about 5×10^5 particles/cm^3. The number of particle distributions at various sizes entering and leaving the ESP are shown in Figure 5. The effect of pulse frequency on the fractional collection efficiency is shown in Figure 6. The pulse frequency was found to play an important role in particle charging. The average number of charges per particle increased rapidly with an increase of pulse frequency. From the figure it can be seen that the collection efficiency at 40 kHz was higher than at 20 kHz, but if the frequency would have been too high, electrical breakdown would have occurred.

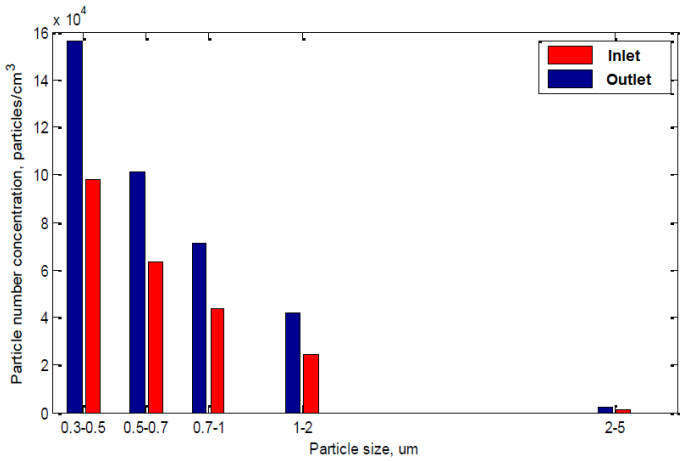

Figure 5 Size distributions of particles at the inlet and outlet of the ESP, operating at a negative pulse voltage of 10kV. Gas velocity was 0.5m/s.

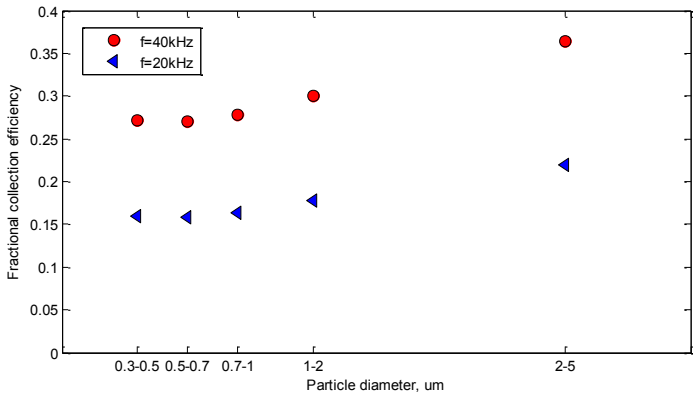

Figure 6 Variation of fractional collection efficiency with particle sizes at various pulse frequencies. Negative pulse peak voltage V_p= 10kV, particle number concentration N =5 × 10^5 particles/cm^3, gas velocity u_g= 0.5m/s.

3.3 Effect of Gas Velocity on Fractional Collection Efficiency

The effect of gas velocity on fractional collection efficiency is shown in Figure 7. The experiments were performed by setting the supplied pulse peak voltage and pulse frequency to be constant at 10 kV and 40 kHz, respectively. The dust loading was controlled at about 5×10^5 particles/cm^3. The gas velocity was adjusted from 0.5 m/s to 2 m/s to provide a gas residence time of 1 s to 0.25 s in the ESP. As shown in Figure 7, it was found that the fractional collection efficiency for the particles sizes of 0.3–5.0 μm increased with the decrease of gas velocity or the increase of residence time.

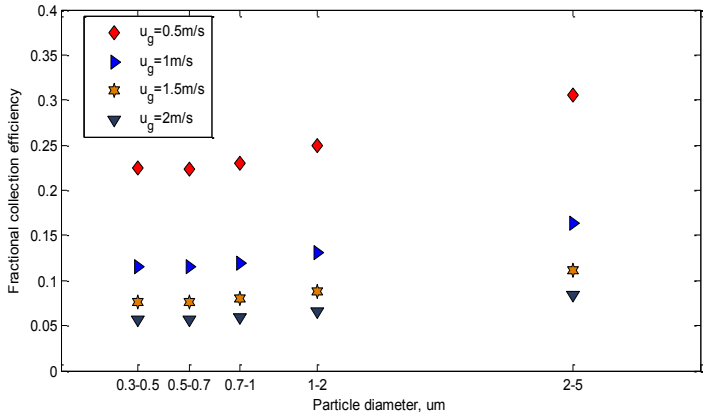

Figure 7 Variation of fractional collection efficiency with particle sizes at various gas velocities. Negative pulse peak voltage V_p= 10 kV, particle number concentration N =5 × 10^5 particles/cm^3, and pulse frequency f = 40 kHz.

3.4 Effect of Supplied Voltage on Fractional Collection Efficiency

Figure 8 shows the effect of the supplied voltage on the fractional collection efficiency. The negative pulse peak was adjusted from 7 kV to 10 kV and 12 kV, while the pulse frequency was kept constant at 20 kHz. Increasing the peak voltage enhanced particle charging, which resulted in a higher collection efficiency. The collection efficiency for particle sizes over 2 μm increased rapidly with the increase of the pulse peak voltage, but only a small gain for particles smaller than 1 μm was obtained due to a difficulty in the electrical charging of very fine particles.

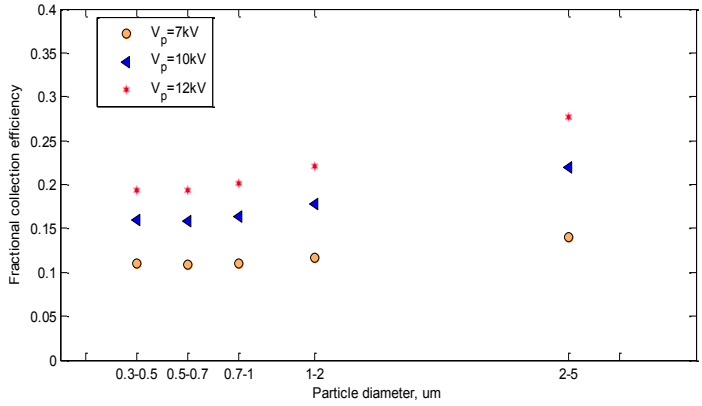

Figure 8 Variation of fractional collection efficiency with particle size at various pulse peak voltages. Pulse frequency f = 20 kHz, particle number concentration N =5 × 10^5 particles/cm^3, and gas velocity u_g= 0.5 m/s.

3.5 Total Mass Collection Efficiency of the ESP for both DC and Pulse Voltage Conditions

Figure 9 shows the total mass collection efficiency of the ESP for both DC and pulsed voltage conditions. The results indicate that the mass collection efficiency increased while the supplied voltage was increased due to the increase of electric field intensity. Unfortunately, for the DC negative voltage, the supplied voltage could not exceed 7 kV due to the electrical breakdown limit. However, for the pulsed voltage conditions, the supplied voltage could go up to 12 kV or higher without electrical spark occurring. Consequently, the mass collection efficiency could be increased up to 92% for pulse frequency at 40 kHz.

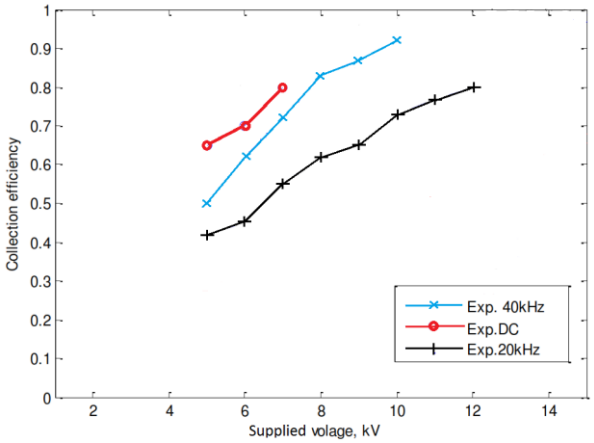

Figure 9 Comparison of collection efficiency for DC ESP and pulse voltage ESP at various pulse frequencies. Gas velocity was 0.5 m/s.

4 Conclusion

An investigation to develop an effective electrostatic precipitator system for the control of soot from diesel combustion was carried out. The following conclusions could be derived.

The wire cylinder ESP with pulsed corona energization indicated a satisfactory collection performance for diesel soot particles. It was found that high voltage pulse energizing not only used lower energy but also had higher efficiency than DC energization.

The total collection efficiency could be increased up to 92% with –10 kV of supplied voltage and a pulse frequency of 40 kHz.

Acknowledgements

The authors would like to acknowledge the Commission on Higher Education, Thailand for the financial support; Rajamangala University of Technology, Lanna, Graduate School and Faculty of Engineering, Chiang Mai University for the testing facilities and other partial supports

References

[1] White, H.J., *Industrial Electrostatic Precipitation*, Addison-Wesley, Reading, MA, 1963.

[2] Thonglek, N., Dechthummarong, C. & Kiatsiriroat, T., *Soot Treatment by Using High Voltage Pulsed Electrostatic Precipitator*, Energy Procedia, **9**, pp. 292-298, 2011.

[3] Fitch, R.A. & Drummond, J.R., *Enhanced Charging of Fine Particles By Electrons in Pulse-Energized Electrical Precipitators*, Physical Science, Measurement and Instrumentation, Management and Education, IEE Proceedings A, **134**(1), pp. 37-44, 1987.

[4] Zukeran, A., Loopy, P.C., Chakrabarti, A., Berezin, A.A., Jayaram, S., Cross, J., Ito, T. & Chang, J.S., *Collection Efficiency of Ultrafine Particles by an Electrostatic Precipitator Under DC and Pulse Operating Modes*, IEEE Trans. Industry Applications, **35**, pp. 1184-1191. 1999.

[5] Xu, D., Sheng, L., Zhai, J. & Zhao, J., *Positive Short-Pulse Corona Discharge Charging of Aerosol Particles*, J. Appl. Phys., **42**, pp. 1-4, 2003.

[6] Xue, F., Luo, Z, Wei, B., Wang, L., Gao, X., Fang, M. & Cen, K., *Electrostatic Capture of PM2.5 Emitted from Coal-Fired Power Plant by Pulsed Corona Discharge Combined with DC Agglomeration*, in Electrostatic Precipitation (the 11th International Conference on Electrostatic Precipitation, Hangzhou, 2008), Prof.Dr. Keping Yan, ed., Springer Berlin Heidelberg, pp. 242-246, 2009.

[7] Sato, S., Kimura, M., Aki, T., Koyamoto, I., Takashima, K., Katsura, S. & Mitzuno, A., *A Removal System of Diesel Particulate Using Electrostatic Precipitator with Discharge Plasma*, Industry Applications Conference, 2005. Fortieth IAS Annual Meeting, Conference Record of the 2005, **3**, pp. 2203-2206, 2005.

[8] Deutsche, W., *Bewegung und Ladung der Elektrizitatstragerim Zylinderkondensator*, Annals of Physics, **68**, pp. 335-344, 1922.

[9] Liu, B.Y.H. & Kapadia, A., *Combined Field and Diffusion Charging of Aerosol Particles in the Continuum Regime*, J. Aerosol Sci., **9**, pp. 227-242, 1978.

[10] Ruttanachot, C., Tirawanichakul, Y. & Tekasakul, P., *Application of Electrostatic Precipitator in Collection of Smoke Aerosol Particles from*

Wood Combustion, Aerosol and Air Quality Research, **11**, pp. 90-98, 2011.

[11] Klippel, N., *The Influence of High-Voltage Pulse Parameters on Corona Current in Electrostatic Precipitators*, J. Electrostatics, **49**, pp. 31-49, 2000.

[12] Grass, N., Hartmann, W. & Klockner, M., *Application of Different of HV Supplies on Industrial Electrostatic Precipitators*, IEEE Trans. Industry Applications, **40**, pp. 1513-1520, 2000.